Unusual Aldehyde Reductase Activity for Production of Full-length Fatty Alcohol by Cyanobacterial Aldehyde Deformylating Oxygenase

Supacha Buttranon
Vidyasirimedhi Institute of Science and Technology
Pattarawan Intasian
Vidyasirimedhi Institute of Science and Technology
Nidar Treesukkasem
Vidyasirimedhi Institute of Science and Technology
Juthamas Jaroensuk
Vidyasirimedhi Institute of Science and Technology
Somchart Maenpuen
Burapha university
Jeerus Sucharitakul
Chulalongkorn University Faculty Of Dentistry
Narin Lawan
Chiang Mai University Faculty of Science
Pimchai Chaiyen
Vidyasirimedhi Institute of Science and Technology
Thanyaporn Wongnate (thanyaporn.w@vistec.ac.th)
School of Biomolecular Science and Engineering, Vidyasirimedhi Institute of Science and Technology (VISTEC), 555 Wangchan Valley, Rayong 21210, Thailand https://orcid.org/0000-0001-5072-9738

Research

Keywords: Non-heme diiron enzyme, Aldehyde-deformylating oxygenase, NADPH-dependent fatty aldehyde reductase, Fatty alcohol, Oxido-reductase

Posted Date: November 5th, 2020

DOI: https://doi.org/10.21203/rs.3.rs-100741/v1

Abstract

Background: Aldehyde-deformylating oxygenase (ADO) is a non-heme di-iron enzyme that catalyzes deformylation of aldehydes to generate alkanes/alkenes. In this study, we report for the first time that under anaerobic or limited oxygen conditions, *Prochlorococcus marinus* (*Pm*ADO) can generate full-length fatty alcohols from fatty aldehydes without eliminating a carbon unit.

Results: Unlike the native activity of ADO which requires electrons from the Fd/FNR electron transfer complex, the aldehyde reduction activity of ADO requires only NADPH. Our results demonstrated that yield of alcohol products can be affected by oxygen concentration and type of aldehyde. Under O_2-scant conditions (10-15%), yields of octanol and dodecanol were around 40-60% and could be increased up to 80% under strict anaerobic conditions (>0.0004%). Unexpectedly, Fe^{2+} cofactor is not involved in the aldehyde reductase activity of *Pm*ADO because yields of alcohols obtained from holo- and apo-enzymes were similar under anaerobic conditions. The direct hydride transfer activity of *Pm*ADO is highly specific to substrates; NADPH not NADH can be used as a reductant to reduce medium-chain fatty aldehydes (C_6-C_{10}) with decanal as the most preferred substrate (the highest k_{cat}/K_m value with 98% bioconversion yield). Molecular dynamics (MD) simulations was used to identify a binding site of NADPH which is located close to the aldehyde binding site. In the metabolic engineered cells containing *Pm*ADO, dual activities of alkane and alcohol production could be detected.

Conclusion: The findings reported herein highlight a new activity of *Pm*ADO which may be applied as a biocatalyst for industrial synthesis of fatty alcohols in the future.

Background

Long-chain alcohols or fatty alcohols are molecules with amphiphilic property. The compounds and their derivatives are valuable and widely used in various industries as commodity chemicals such as detergents, surfactants, additives, personal care products, etc [1-5]**.** The global production of fatty alcohol was above three million tonnes in 2015 [5]. Currently, fatty alcohols can be produced from petroleum-based resources *via* ethylene polymerization and oxidation [6] or from bio-based materials such as triglyceride from palm oil industry via transesterification and hydrogenation [7, 8] .Current methods for production fatty alcohols from both petro-based and bio-based materials are chemical processes which are not green and lead to high amount of CO_2 emission [9]. Currently, industrial scale production of many valuable compounds including bio-alcohols from renewable feedstocks are possible due to advancement in synthetic biology, metabolic engineering and bioprocess [10-12]. New and efficient biocatalysts for fatty alcohol production will contribute towards development of their production *via* bioprocess from renewable feedstocks which will help transform industries towards UN's sustainable development goals [9, 10].

Several metabolic pathways and various types of microorganisms have been engineered for production of fatty alcohols [1, 2, 13-15]. However, the limitation lies at the production level of fatty alcohols which

are required to increase titers, yields, productivities, and robustness in large-scale industrial process, making microbial production more cost-effective and commercially viable. Most of these engineered pathways rely on one-step or two-step reduction processes. The one-step reduction system uses the enzyme fatty acid reductase (FAR) to reduce fatty acyl ACP/CoA directly to yield fatty alcohols. The two-step reduction system uses two enzymes in which the first step is reduction of fatty acyl ACP/CoA by fatty acyl ACP/CoA reductase (AAR/ACR) or reduction of free fatty acid by carboxylic acid reductase (CAR) to yield fatty aldehyde [16-20]. The resulting fatty aldehyde is further converted to fatty alcohol by aldehyde reductase. However, high activities were observed for selected alcohols such as 1-propanol, 1-butanol, 1-pentanol, isoamyl, 1-hexanol, 1-octanol, and benzyl alcohols with relatively high K_m values [21]. Alternatively, if the engineered microbe contains a gene encoding an aldehyde-deformylating oxygenase (ADO), end product of the pathway is alkane/alkene instead of fatty alcohol [22, 23]. It has previously been reported that ADO can also convert fatty aldehydes to fatty alcohols with one-carbon less (C_{n-1}) as a side reaction in very low yields [24]. It is currently unclear how ADO can catalyze one-carbon atom elimination and aldehyde reduction to produce fatty alcohols.

Aldehyde-deformylating oxygenase (ADO) from cyanobacteria *Prochlorococcus marinus* (*Pm*ADO) is a non-heme diiron enzyme catalyzing the O_2-dependent production of one carbon less (C_{n-1}) alkanes/alkenes from aldehydes [25]. This enzyme has been attractive for applications in metabolic engineering to produce hydrocarbon [22, 23, 26]. ADO belongs to the ferritin-like di-iron proteins superfamily [27, 28], in which both iron atoms are coordinated with two histidine and four glutamate residues [25, 29-31]. In order to catalyze alkane production, molecular oxygen (O_2) and reductant (either in the form of an electron transfer system such as reduced ferredoxin generated from ferredoxin reductase or chemical reductant such as phenazine methosulfate) are required for ADO activity [25, 32-35]. The iron-peroxo species generated by the interaction of O_2 and irons is responsible for attacking aldehyde substrate to form the hemiacetal intermediate, which is subsequently converted to the corresponding products alkane and formate [25, 33-37]. Based on sequence similarity and three- dimensional structures, ADO belongs to the class of enzymes that utilize diiron to activate O_2 including ribonucleotide reductase (RNR) [22, 38-40] methane monooxygenase (MMO) [41, 42] tRNA-modifying enzyme (MiaE) [43], fatty acid desaturase [44], and toluene monooxygenases (TMO) [45-47].

Reaction mechanisms of these enzymes proceed via an oxygen-activation process to generate a reactive radical intermediate. Oxygen binding is indispensable to these enzymes. However, the proposed peroxo intermediates binding mode was predicted based on structural characterization [48] and remains a subject of debate. Isotope labeling studies of the enzyme from *Nostoc punctiforme* show that one O atom in the formate product is derived from O_2 [34]. This result is explained as the attack of the nucleophilic peroxo intermediate on the electrophilic carbon atom of the aldehyde substrate to initially form a peroxy hemiacetal. In support of this mechanism, an intermediate arising from a peroxo band has been trapped [48]. Studies of the ADO from *Prochlorococcus marinus* with C8–10 aldehydes show formation of the expected C7–9 alkane as well as the corresponding primary alcohol and aldehyde in very

low yields. Therefore, the role of oxygen in ADO reaction and reaction mechanism of alkane and alcohol products formation are still not clear.

Here, we found a novel activity of *Pm*ADO to generate full-length fatty alcohols, not one-carbon less, from aldehydes instead of alkane. The reaction mechanism of this aldehyde reductase activity and the role of oxygen and Fe^{2+} cofactor was investigated. We first explored fatty alcohol production in the metabolic engineered cell carrying the ADO gene. We found that in addition to alkanes, the cell containing ADO generated fatty alcohols in significant amount. We investigated in-depth how fatty alcohol can be generated by ADO using the purified ADO and the reconstituted system of ADO and redox partners. The results showed that ADO can produce fatty alcohols from fatty aldehydes without requiring O_2, metals and canonical redox partners such as ferredoxin/ferredoxin reductase (Fd/FNR) or phenazine methosulfate (PMS). Our work is the first study to report that under O_2-limited conditions, *Pm*ADO exhibits NADPH-dependent reductase activity which mainly catalyzes direct hydride transfer from NADPH to fatty aldehydes to produce fatty alcohols in the full-chain form. It should be noted that this activity is different from the previous results reporting very small amount of one-carbon less fatty alcohol production. The new aldehyde reductase activity of ADO is high and efficient, suggesting it's promising potential in production of fatty alcohols *via* bio-process in the future.

Results

Production of fatty alcohols by *E. coli* cells containing ADO

As illustrated in the previous report, alkane production can be produced from the synthetic metabolic pathway in *Escherichia coli* having aldehyde deformylating oxygenase (ADO) from *Prochlorococcus marinus* MIT9313, fatty acyl-CoA reductase (ACR1) from *Acinetobacter baumannii* and associated with redox partners ferredoxin (Fd) from *Synechocystis* sp. PCC 6803, ferredoxin (flavodoxin): $NADP^+$ oxidoreductase (FNR). It was shown that addition of formate dehydrogenase (FDH) from *Xanthobacter* sp. 91 could increase intracellular NADH/NAD^+ ratio in cells which can increase higher level of reduced Fd and increase yield of alkane production ~50% (23). Here, we further explored why the alkane product was limited at ~50% by further exploring whether this cell can generate other types of by-products. Analysis of metabolite profiles of the engineered cells containing *Pm*ADO and various types of auxiliary systems indicated that these cells produced significant amount of fatty alcohol, up to 25% fatty alcohols (Figure 1). This result prompted us to explore in-depth reaction mechanisms of fatty alcohol formation by *Pm*ADO using the purified enzyme and reconstituted systems.

Fatty alcohol production by the purified *Pm*ADO

Based on the results above showing that the metabolic engineered cell overexpressing *Pm*ADO could produce significant amount of fatty alcohol, we thus explored aldehyde reductase activity of the purified *Pm*ADO and also carried out experiments to rule out possible involvement of contaminating aldehyde reductases from the *E. coli* cell. As shown in Figure 2, the *Pm*ADO (with a subunit molecular weight of 24

kDa) obtained from our purification process (Experimental Procedures) is highly pure (>98% purity) with no other protein contamination visible by SDS-PAGE analysis. Based on the *E. coli* genome sequence, we identified putative aldehyde reductases produced in cells to monitor whether they could introduce possible false reductase activity in our *Pm*ADO assays. The analysis summarized in Additional file 1: Table S1 indicates that other genes identified as reductases (yahK, frmA, adhE, adhP, eutG, yqhD, yiaY and yjgB) all have their protein subunit sizes around 35-96 kDa. Results in Figure 2 clearly show that the purified *Pm*ADO obtained from our preparation has no (not even trace amount) contaminating protein in that region, ruling out a possibility of having other aldehyde reductases present in our enzyme sample. Using assays described in Experimental Procedures and in Table 1, the results indicated that the purified *Pm*ADO could catalyze fatty alcohol production from fatty aldehyde using various reducing systems (more results discussed below).

Fatty alcohol production by the unusual reaction of *Pm*ADO reductase activity

We first figured out nature of reductant required for *Pm*ADO aldehyde reductase activity and the effect of oxygen on this reaction. Reaction mixtures containing dodecanal and various $\%O_2$ (<0.0004%, 10%, and 15%) in the presence or absence of a reducing system, which are ferredoxin and ferredoxin reductase (Fd/FNR) were analyzed by GC/MS. Amount of fatty acid, alkane and alcohol products produced under various concentrations of oxygen and the reducing systems are shown in Table 1. The alcohol production by *Pm*ADO decreased when the O_2 concentration was increased. The highest alcohol production was observed under anaerobic conditions with less than 0.0004% oxygen for both systems of *Pm*ADO with NADPH and *Pm*ADO with NADPH and Fd/FNR (Table 1). We noted that the alcohol production was not observed in the reactions without NADPH (Additional file 1: Figure S1).

Interestingly, dodecanal could be converted to dodecanol by *Pm*ADO in the absence of ferredoxin and ferredoxin reductase. The results showed that alcohol production yield by *Pm*ADO with NADPH (69 ± 5 μM) exhibited a similar value of product to the reaction of *Pm*ADO with the Fd/FNR reducing system (75 ± 4 μM) at less than 0.0004% O_2 (Table 1). In the presence of the reducing system (Fd/FNR), the *Pm*ADO reaction showed an increase in alkane along with acid production when oxygen was increased (Table 1). However, the reaction of *Pm*ADO without the ferredoxin and ferredoxin reductase showed only acid in addition to the alcohol product (Table 1). These results indicate that the Fd and FNR are not necessary for transferring electrons from NADPH to produce alcohol by *Pm*ADO. Notably, *Pm*ADO can convert aldehydes to n-alcohols in the presence of only NADPH. As the highest yield could be obtained under anaerobic conditions, the data suggest that O_2 is not necessary for the production of fatty alcohol by *Pm*ADO. Therefore, a minimum system for production of alcohol by *Pm*ADO only requires aldehyde and NADPH substrates (Scheme 1). Factors affecting production of fatty alcohol from aldehyde by *Pm*ADO including reducing systems and O_2 concentrations are summarized in Table 1 and Figure 3.

To further address the effects of oxygen on production of fatty alcohol and to fine tune conditions for maximum alcohol production, reactions were performed in an anaerobic glove box and pre-incubated with an oxygen scavenging system glucose and glucose oxidase (Glc/GOx) to completely remove

oxygen. Under these conditions and using octanal as a substrate, the detected octanol (80% conversion) was 20% greater than that of the reaction without oxygen scavenging system (60% conversion) (Figure 3B). Accordingly, no heptane or octanoic acid could be detected in these reaction mixtures. These data solidly demonstrate the conversion of fatty aldehyde to yield 80% fatty alcohol by aldehyde reductase activity of *Pm*ADO using NADPH as an electron donor in the absence of O_2 and other redox partners.

To explore specificity of reducing equivalent for aldehyde reductase activity of *Pm*ADO, we investigated whether the enzyme can use NADH in addition to NADPH. The result showed that the *Pm*ADO aldehyde reductase activity could only use NADPH not NADH to produce fatty alcohol (Figure 4). Even with increased concentrations of *Pm*ADO (20, 40, 80, and 160 μM) in the presence of NADH, none of the reactions could produce fatty alcohols (Additional file 1: Figure S2).

The above findings showing that the purified *Pm*ADO could only use NADPH as a reductant also ruled out a possibility that the aldehyde reductase activity observed in this report comes from contamination of other aldehyde reductases produced in *E. coli* cells. Most of aldo–keto reductases in *E. coli* are known to use both NADPH and NADH as reductants to reduce a variety of aldehydes and carbonyl moieties [34, 46-49] (Additional file 1: Table S1). The only aldehyde reductase in *E. coli* which can use NADPH as a reductant is yqhD (Additional file 1: Table S1). As a subunit molecular weight of yqhD is 42 kDa, this indicates that the purified *Pm*ADO with a subunit molecular weight of 24 kDa (Figure 2) has no contamination from yqhD or other aldehyde reductases from *E. coli*. Altogether, all data suggest that the aldehyde reduction by NADPH was indeed catalyzed by the purified *Pm*ADO.

A ferrous (Fe^{2+}) ion is not necessary for the aldehyde reductase activity of *Pm*ADO

The role of metal cofactor in aldehyde reductase activity of *PmADO* was investigated. We explored the involvement of Fe^{2+}-cofactor in this activity by preparing an apoenzyme form of *PmADO* and measured its activity in comparison with Fe^{2+}-bound holoenzyme. Although the native O_2-dependent ADO reaction is involved with formation of an iron (III)-peroxo intermediate [34, 50] ,the aldehyde reductase activity to generate fatty alcohol is not involved with the metal cofactor and may not require the diiron-cofactor. Results from comparison of activities of ferrous supplemented *Pm*ADO, holo-*Pm*ADO and apo-*Pm*ADO (Figure 5) showed that the yield of fatty alcohol production from holo-*Pm*ADO (~60%) was similar to that observed in the reaction of apo-*Pm*ADO (~55%) and adding extra Fe^{2+} to the reaction (~75%). Based on standard variations of measurements, these values are all in the same range. Here, the results indicate that the metal cofactor is not involved in the reductase activity of *Pm*ADO. The MD simulations results (discussed later) also confirmed this conclusion.

The reductase activity of *Pm*ADO is highly specific towards medium- to long-chain aldehydes

Specificity of aldehydes that can be reduced by *Pm*ADO was investigated by carrying out the reactions of *Pm*ADO with medium- and long-chain (C_6, C_8, C_{10}, C_{12}, and C_{14}) aldehydes and analyzed for alcohol production (Table 2, Figure 6). Based on kinetic parameters, the results indicate that *Pm*ADO does not

exhibit strong chain length specificity with aldehyde substrates. This feature is consistent with specificity of aldehyde usage in the native *Pm*ADO activity in which both native cyanobacteria and reconstituted *Pm*ADO systems in *E. coli* can generate a wide range of alkane products [25, 51]. The results show that conversion of decanal to decanol gave the highest yield (98%) among all substrates used. Percentages of other aldehyde conversion to alcohol products were 86%, 79%, 68%, and 70% for hexanal, octanal, dodecanal, and tetradecanal, respectively. k_{cat} and K_m values of hexanal, octanal, and decanal are all relatively similar with a moderate trend of decreasing K_m with increasing chain length of aldehyde from C_6 to C_{10} (10.8 μM for C_6, 10.3 μM for C_8, and 6.5 μM for C_{10} (Table 2)). On the contrary, for the case of C_{12} and C_{14}, the K_m value increases with increasing chain length (Table 2); k_{cat} of C_{12} is higher than that of C_{14}. Altogether, these trends contribute to an approximately 3- to 5-fold changes in reaction efficiency (k_{cat}/K_m) from 15×10^{-3} $\mu M^{-1}min^{-1}$ for C_{10} to 3×10^{-3} $\mu M^{-1}min^{-1}$ for C_{12} and 5×10^{-3} $\mu M^{-1}min^{-1}$ for C_{14} (Table 2). It is important to note that no alcohol production was observed when 2-octenal was used as a substrate (Additional file 1: Figure S3).

Molecular docking and molecular dynamics (MD) simulations to identify a putative NADPH binding site

In order to identify a putative NADPH binding site in *Pm*ADO, MD simulations was used to dock NADPH and aldehyde into the *Pm*ADO active site. As decanal gave the highest catalytic efficiency in alcohol production by *Pm*ADO (Table 2), decanal was chosen to use in molecular docking and MD simulations studies. A structure of decanal was generated based on the structure of 11-[2-(2-ethoxyethoxy) ethoxy undecanal, which could be co-crystallized as a ligand in the *Pm*ADO crystal structure (PDB code 4PGK). NADPH was placed into the system containing *Pm*ADO and decanal. MD simulations were used to release stain of the protein and explore NADPH binding at the active site with the lowest energy point (-8.4 kcal/mol). The results showed that NADPH could bind to helices 1, 2, 4, and 5, which are close to the aldehyde binding site of *Pm*ADO. Snapshots taken around 0.54 ns of MD simulations are shown in Figure 7A. Moreover, the MD simulations also indicated that distances between C_α of Glu73 and C_α of Glu157 changed over the course of MD simulations, representing open and close forms of the *Pm*ADO enzyme. The open form could be observed before 0.54 ns (C_α of Glu73 and C_α of Glu157 bond distance increased from 12 to 20 Å) while the semi-closed form occurred after 0.54 ns (C_α of Glu73 and C_α of Glu157 bond distance decreased from 20 to 14 Å) (Figure 7B). These dynamics may represent the *Pm*ADO:NADPH:aldehyde complex conformational change prior to the next reduction step.

Additionally, the MD simulations of the *Pm*ADO:NADPH: decanal complex identified the distance between the C4-position of hydrogen atom of NADPH and the carbonyl carbon of fatty aldehyde (Figure 7A) as 3.8 Å. With this binding mode, the enzyme-bound NADPH can make stable contacts with decanal in the binding site of the *Pm*ADO. It should be mentioned that the *Pm*ADO structure used in our MD simulations (PDB code: 4PGK) was solved under aerobic conditions which may not represent the structure relevant to aldehyde reductase activity reported here. A hydride transfer distance in this structure may not be close enough for aldehyde reduction to occur. Up to now, no anaerobic crystal structure of an ADO enzyme is available. In the presence of molecular oxygen, the active site might be blocked, and consequently

prohibiting the reaction between NADPH and aldehyde. In the case of aldehyde reductase, it is known that the hydride transfer from a nicotinamide co-substrate occurs only with a dehydrated aldehyde [52]. As aldehyde in solution likely exists in the hydrated form, thus during binding of a substrate, water must be stripped away for the substrate to prompt the compound for the catalysis [53]. This phenomenon explains the superiority of anaerobic alcohol production by ADO enzyme because molecular oxygen was removed for a proper binding of the enzyme substrate complex. The unique activity of *Pm*ADO that directly reduces fatty aldehyde by NADPH under anaerobic conditions provides structural and functional insights of *Pm*ADO for future biotechnology applications.

The reductase activity of recombinant *Pm*ADO enhances alcohol production in the metabolically engineered cell

To demonstrate the fatty alcohol production from reconstituted *Pm*ADO in *E. coli* under limited oxygen concentration, the *Pm*ADO and carboxylic acid reductase from *Mycobacterium marinum* (MmCAR) were constructed and measured fatty alcohol production in the metabolic engineered cell. MmCAR can catalyze fatty acid to aldehyde. Then, *Pm*ADO can use fatty aldehyde as a substrate to produce fatty alcohol. In order to avoid complications, decanoic acid was used as a supplement. The plasmids consisting of only MmCAR were also constructed to investigate the native aldehyde reductase activity from endogenous aldehyde reductase (AHR) in *E. coli*. Both plasmid systems were expressed in *E. coli* and the production of alcohol was quantified by GC/MS after 6 hours of a bioconversion process under various oxygen concentrations (<0.0004, 5, 10, 15, 20%). The results showed that fatty alcohol production could be observed in both MmCAR and MmCAR+*Pm*ADO under all oxygen concentrations (Figure 8). However, fatty alcohol production in the cell harbouring MmCAR+*Pm*ADO showed much greater amount of product than that of MmCAR cell factory, approximately 2-fold under almost all oxygen concentrations. The exception was found for the condition with <0.0004% O_2 because both cell types showed low alcohol production (22%). This might be due to the disruption of energy metabolism in *E. coli* cells under strict anaerobic conditions [54]. Under 5% oxygen, MmCAR+*Pm*ADO gave the highest alcohol yield of dodecanol which is about 75%. This finding demonstrates that *Pm*ADO has the ability to enhance alcohol production in a cell factory as well as *in vitro*.

Discussion

Our work here found a new activity of *Pm*ADO which has not been documented. *Pm*ADO was reported to convert aldehyde to alkane or alkene under aerobic conditions [24], and alcohol products with one-carbon less could also be generated. ADO typically requires a reducing system to produce alkane or alkene [50]. However, when the reaction contains extra O_2, the reaction sometimes proceeds through the formation of acid in addition to alkane [50]. The previous study has shown that ADO under fully aerobic conditions showed comparatively low activity. However, under micro-aerobic (3-10% O_2) conditions, ADO could carry out the reaction for maximum of 3 turnovers with dodecanal as a substrate [55]. Moreover, O_2 is strictly required for bioconversion to produce the n-1 carbon alkane products along with n-1 aldehyde and n-1 alcohol. Previously, it was shown that only 2% of heptanol could be produced from octanal [24]. The

system strongly requires O_2 to produce n-1 aldehyde and n-1 alcohol because of the reaction mechanism involved [24]. Under our investigation, the reactions which were run in an anaerobic chamber following preincubation with oxygen scavenging system also did not detect any n-1 alcohol products, consistent with the previous finding. However, we detected full-length alcohol products which were not previously reported.

In this context, our findings here of full-length fatty alcohol products and that *Pm*ADO does not require dioxygen or canonical reductant (Fd/FNR) nor di-iron cofactor for alcohol production but only requires a hydride transfer from NADPH were unexpected. The results obtained prompted us to explore the peculiar activity of *Pm*ADO in fatty aldehyde reduction by a direct hydride transfer process under anaerobic conditions. We found that *Pm*ADO could convert aldehydes into full-length alcohols up to 80% yield under a condition containing O_2-scavenging system. Analysis by MD simulations of NADPH binding with *Pm*ADO also support the binding of this ligand (Figure 7). The substrate-binding site of ADO comprises a long hydrophobic channel that terminates at the di-iron centre [55]. Similar to other aldehyde reductase (AHR) crystal structues, the binding cavity comprises hydrophobic pockets which can accommodate a nicotinamide ring and aldehyde substrate [56]. Recently, the active-site residues have been identified and showed that the residues close to the di-iron centre exerted influence on ADO activity [57].

This novel reduction reaction is also different from the native deformylation reaction of *Pm*ADO on the substrate specificity. The reduction reaction shows almost full conversion (98%) only with medium chain aldehydes. In the case of deformylation reaction, it shows broad substrate specificity in all long- and short-chain aldehydes; octadecanal and heptanal, were used as substrates for ADO almost equally well [25, 28, 29, 33-36, 58, 59]. Based on the co-crystal structures of cyanobacterial ADO with substrate analogues [22, 30], changes of the amino acids close to the aldehyde binding site and the hydrophobic tail of the substrate and those along the substrate channel may affect the substrate specificity [60]. Moreover, the structures of ADO demonstrated that several modes of binding are possible for aldehydes. In the case of short-chain aldehydes, more than one molecule has been proposed to bind in the ADO substrate cavity [24]. These results suggest that non-productive substrate binding modes might be present. It was, then, hypothesized that the location of NADPH might be a key factor to increase medium-chain aldehyde interaction in *Pm*ADO active site and promote the hydride transfer, which is supported by the highest k_{cat}/K_m of 250 $M^{-1}s^{-1}$ with 98% conversion of decanol. The biosynthesis of fatty alcohol by thioesterases has been investigated in the production of various chain length alcohols [1, 17-19, 32]. However, the aldehyde reductase, which is responsible for reduction of specific chain length aldehydes to alcohol, remains unclear. In the case of yjgB [32] and yqhD [1], these enzymes demonstrated improvement in long-chain alcohol production. Nevertheless, the enzymes that play major roles for conversion of long-chain aldehyde into alcohol is yet to be clarified. Therefore, the knowledge obtained from this study will be useful in designing new efficient biocatalysts for the production of fatty alcohols.

Previous studies of the metabolic engineering for alkane biosynthesis using ADO all showed that the alkane production yield was less than 50% [12, 16, 23, 32, 61-64]. This might be due to the fact that ADO could produce both alkane and fatty alcohol, diverting the yield of alkane biosynthesis. Apart from

production by ADO, the metabolic engineered cells containing aldehyde producing enzymes can also generate fatty alcohols from endogenous aldehyde reductases (Figure 1) [8, 16, 62]. Our studies demonstrated that yield of fatty alcohol products in whole cell biocatalysis can be affected by oxygen concentration. Under 10-20% O_2, yields of decanol was around 60-70% and could be increased up to 75% under 5% O_2 which is 58% higher than that of endogenous aldehyde reductase strain. Therefore, the metabolically engineered cells such as those demonstrated in Figure 8 can be employed as biocatalysts with dual and tunable activities. Our knowledge here suggests that in the future, the same cells can be tuned for production of alkane or fatty alcohol depending on bioconversion conditions.

Conclusion

In this work, we have shown for the first time that *Pm*ADO exhibits unusual activity to reduce fatty aldehydes to fatty alcohols by a reduction process using only NADPH as an electron donor under O_2-limitted conditions. This feature makes *Pm*ADO a more versatile catalyst than previously recognized. It is possible to use the enzyme for alcohol production by providing the enzyme with aldehyde and NADPH under anaerobic conditions. This phenomenon requires NADPH to donate a hydride to aldehyde to generate alcohol, in which up to 80% fatty alcohol could be produced in the reactions containing O_2-scavenger system while supplementing Fe^{2+} to the *Pm*ADO reaction showed no significant impact on alcohol production. *Pm*ADO revealed a wide range of aldehydes that can be used as substrates. The activity suitable for the medium-chain aldehyde usage could yield up to 98% conversion and showed very high k_{cat}/K_m (250 $M^{-1}s^{-1}$). Moreover, MD simulations confirmed that NADPH can bind to the active site of the *Pm*ADO, which is close to the aldehyde binding site with binding energy of -8.4 kcal/mol. The MD simulations results also showed that NADPH has stable contacts with aldehyde in the binding site of the *Pm*ADO. Moreover, *Pm*ADO can enhance the alcohol production in a cell factory, making the cell having dual activities for both alkane and alcohol production. These findings open a new biocatalytic application of *Pm*ADO in terms of fatty alcohols production.

Materials And Methods

Chemicals and reagents

All chemicals were commercially available and of high quality and analytical grade. Oligonucleotides and the gene encoding ADO from Prochlorococcus marinus (strain MIT 9313) (pmado) were synthesized and codon optimized by the GenScript Biotech Corp. (China). Restriction endonucleases NdeI and BamHI were from New England BioLabs.

Strain and plasmids construction

E. coli XL1-Blue and *E. coli* BL21 (DE3) from Novagen were used as cloning and protein expression strains, respectively. pET17b, pCDFduet-1 and pRSFDuet-1 vectors were applied for construction. The same plasmid sets as the previous study [23] were used to investigate alcohol and alkane production by

*Pm*ADO in whole-cell catalysts (pET17b-acr1, pCDFDuet-1-fd-fnr-pmado, pRSFDuet-1-trxA-trxB and pRSFDuet-1-fdh). To investigate further about the ability of *Pm*ADO for fatty alcohol production, pET17b-mmcar and pCDFDuet-1-pmado were used in whole-cell bio-catalysis assays.

In vivo fatty alcohol production by whole-cell biocatalysis

E. coli BL21 (DE3) cells harboring each set of gene constructs were used for alkane and fatty alcohol production (pET17b-acr1, pCDFDuet-1-fd-fnr-pmado, pRSFDuet-1-trxA-trxB and pRSFDuet-1-fdh). To determine the ability of *Pm*ADO to produce alcohol, cells containing pET17b-mmcar/pCDFDuet-1-pmado and pET17b-mmcar were cultured in 5 mL of LB medium contain 100 µg/ml ampicillin or 25 µg/ml streptomycin at 37 °C for 16 hours. A 1% (v/v) inoculum of bacterial culture was further cultured in 150 mL of terrific broth at 37 °C. Until OD_{600} of the culture reached about 0.5, the temperature of the culture medium was lowered to 25 °C. Then, 1 mM isopropyl-b-D-glucopyranoside (IPTG) was added and the culture was maintained at this temperature for 8 hours. The cell paste was resuspended and adjusted cell density to OD_{600} of 20 in 100 mM potassium phosphate buffer pH 7.5 supplemented with 2.5% glucose, and 0.85 mM tetradecanoic acid.

In experiments with various oxygen concentrations, the harvested cell paste was resuspended inside an anaerobic glover box and adjusted cell density to OD_{600} of 20 in 100 mM potassium phosphate buffer, pH 7.5 containing 0.8 mM decanoic acid. The resuspension was adjusted with various O_2 concentration (<0.0004, 5, 10, 15 and 20%). Then, the suspension was incubated at 25 °C for 6 hours. Samples were collected, extracted by ethyl acetate separation, and analyzed by GC/MS for quantitation of decanol product.

Enzyme expression and purification

Escherichia coli BL21(DE3) cells harbouring pET17b-pmado were cultured in a ZYM-5052 auto-induction rich medium containing 50 µg/mL of ampicillin, and 1X 5052 medium at 37 °C until OD_{600} of the culture reached approximately 1. Then, the temperature of the culture medium was adjusted to 25 °C and maintained at this temperature for 6-8 hours to overexpress *Pm*ADO. *Pm*ADO was purified to homogeneity using precipitation methods (0.5%(w/v) PEI and 40-60%(w/v) $(NH_4)_2SO_4$ precipitation) and anion-exchange column chromatography (DEAE-Sepharose). The purity of *Pm*ADO after purification was analyzed by 12%(w/v) SDS-PAGE, which identified its subunit molecular weight as 24 kDa (Figure 2). Most of molecular weights of endogenous aldehyde reductases commonly found in *E. coli* BL21(DE3) are larger (35-96 kDa) than 24 kDa.

For overexpression of the reducing systems (Fd and FNR), the expression constructs of pCDFDuet-1 plasmid conjugated with the fd gene from Synechocystis sp. PCC 6803 and modified with 6xHis on N-terminus (pCDFDuet-1-fd) and the fnr gene from *E. coli* K-12 (pCDFDuet-1-fnr) were overexpressed in *E. coli* BL21(DE3) cells cultured in LB medium containing 25 µg/mL streptomycin at 25 °C for 6-8 hours with the addition of 1 mM IPTG to induce protein production. Fd was purified to homogeneity using

precipitation methods (0.1%(w/v) PEI and 0-10%(w/v) $(NH_4)_2SO_4$ precipitation) and affinity column chromatography (Nickel-chelating Sepharose). The purity of Fd after purification was analyzed by 14% (w/v) Tricine SDS-PAGE which determine its subunit molecular weight as 9.4 kDa. FNR was purified to homogeneity using precipitation methods (1%(w/v) PEI and 40-80%(w/v) $(NH_4)_2SO_4$ precipitation) and anion-exchange column chromatography (DEAE-Sepharose). The purity of FNR after purification was analysed by 12%(w/v) SDS-PAGE, which determine its subunit molecular weight as 27 kDa.

Activity assay and product analysis

Activity assays were performed in 100 mM HEPES buffer, pH 6.8, containing 100 mM KCl. Aldehyde substrates (C_{6-14}) were prepared as a 10 mM stock solution in methanol. A typical assay contained 10 µM *Pm*ADO, 250 µM aldehyde substrate and 1 mM NADPH. To study the effect of the reducing system on alcohol production by *Pm*ADO, 10 µM Fd, and 10 µM FNR were added into the reaction. The assay reactions were placed at 37 °C, quenched by addition ethyl acetate in a 1:1 ratio, and vigorously vortexed before centrifugation at 13,800 ´g and 4 °C for 10 min. The clear organic phase was analysed by gas chromatography/mass spectrometry (GC/MS) using a HP-5 column, and the column was continuously flown with a He gas at a constant flow rate of 7 ml/min and 250 °C injection port. The sample was split at the mass spectrometer (GC/MS) using the following oven temperature programme: 60 °C held for 3 minutes, 200 °C held for 2 min, and 260 °C held for 3 min at 10 °C min^{-1} and 20 °C min^{-1}. Concentrations of products were determined by a standard curve.

Effects of oxygen and the reducing system on alcohol production by *Pm*ADO

The effects of oxygen on the *Pm*ADO activity were assessed inside an anaerobic glove box (<0.0004% O_2, Belle Technology, UK) to avoid the disturbance of oxygen in air. The alcohol product yielded by *Pm*ADO reaction containing various concentrations of oxygen, <0.0004 (mostly anaerobic), 10, and 15%, and in the absence and presence of the reducing systems (Fd/FNR) was analysed by GC/MS as described above. To deplete oxygen completely, the reaction buffer was pre-incubated with an oxygen-scavenging system, 200 µM glucose and 10 µg/ml glucose oxidase (Glc/GOx) before the reaction started.

Effect of metal cofactor on alcohol production of *Pm*ADO

The metal contents in the purified *Pm*ADO were determined using an inductively coupled plasma optical emission spectrometer (ICP-OES). Apoenzyme of *Pm*ADO (apo-*Pm*ADO) was prepared by either incubating *Pm*ADO with a 5-fold excess concentration of EDTA or treating the enzyme solution with Chelex 100 chelating gel (Bio-Rad Laboratories, Inc., USA) overnight, and the EDTA-metal complexes were removed by a PD-10 (Sepahdex G-25) desalting column pre-equilibrated with 100 mM HEPES buffer, pH 6.8, containing 100 mM KCl that was prepared from a Milli-Q® Type 1 ultrapure water. The eluted apoenzyme was collected, and the protein concentration of apo-enzyme was determined at 280 nm (ε= 17,545 $M^{-1}cm^{-1}$).

Substrate specificity

A solution of C_6, C_8, C_{10}, C_{12}, and C_{14} aldehyde substrate (250 μM) was mixed with 10 μM *Pm*ADO and 1 mM NADPH in 100 mM HEPES buffer, pH 6.8, containing 100 mM KCl under anaerobic conditions using the Glc/GOx scavenging system in anaerobic glove box. The corresponding alcohol products were characterized by GC/MS.

Kinetics measurement

Kinetics assays were performed at 25 °C in 100 mM HEPES buffer, pH 6.8, containing 100 mM KCl under anaerobic conditions. The reaction assays contained 8 μM *Pm*ADO, 200 μM NADPH, and various concentrations of C_6, C_8, C_{10}, C_{12}, and C_{14} aldehyde substrates (10-300 μM). The rate of NADPH consumption detected at absorbance 340 nm represented *Pm*ADO activity. One unit of *Pm*ADO activity was defined as 1 μmol NADPH consumed per min at pH 6.8 and 25 °C.

Computational details

ADO was MD simulated in order to release strain in the protein structure. Molecular docking was carried out in order to identify a putative NADPH binding site. The ADO enzyme structure was obtained from the Protein Databank (PDB) with code 4PGK [65]. Hydrogen atoms of amino acid residues were added by considering results from the PropKa [66]. The atom types in the topology files were assigned based on the CHARMM27 parameter set [67]. The structure of ADO enzyme was solvated in a cubic box of TIP3P water extending at least 15 Å in each direction from the solute. Dimension of the solvated system is 70 x 75 x 84 Å. In this work, MD simulations were carried out by using NAMD program [68] with simulation protocols adapted from previous work [69] and NAMD tutorials [70, 71]. The simulations were started by minimizing hydrogen atom positions for 3,000 steps followed by water minimization for 6000 steps. The system water was heated to 300 K for 5 ps then was equilibrated for 15 ps. The whole system was minimized for 10,000 steps and heated to 300 K for 20 ps. Then, the whole system was equilibrated for 180 ps followed by production stage for 4 ns.

Abbreviations

ADO, Aldehyde Deformylating Oxygenase; *Pm*ADO, ADO from *Prochlorococcus marinus*; NADPH, Nicotinamide Adenine Dinucleotide Phosphate; *Mm*CAR, Carboxylic acid reductase from *Mycobacterium marinum*

Declarations

Ethics approval and consent to participate

Not applicable.

Consent for publication

Not applicable.

Competing interests

The authors declare that the contents of this article have been filled for patent application.

Funding

This work was supported by The Mid-Career Research Grant 2020 from National Research Council of Thailand (to T.W. and S.M.).

Authors' contributions

SB, PI, NT, JJ, SM, JS, NL, PC, and TW designed experiments. SB, NT, JS, and SM expressed and purified all protein and enzymes. SB and PI performed and analyzed ADO activity and products. SB and JS preformed and analyzed effects of oxygen and metal on alcohol production of ADO. SB and NT preformed and analyzed substrate specificity. NL performed molecular dynamics simulations. SB and TW drafted a manuscript. SB, JJ, SM, JS, PC and TW corrected and shaped up the manuscript.

Acknowledgements

We also thank funding support from Vidyasirimedhi Institute of Science and Technology (VISTEC), Global Partnership Program from Program Management Unit-B and Royal Academy of Engineering (UK) for S.B., N.T., J.J., P.I., P.C. and T.W and Chiang Mai University for N.L. The Thailand Research Fund grant number RSA5980062 and targeted research funding and integration for research group development to become specialized center (to J.S.).

Availability of data and material

The datasets used and/or analyzed during the current study are available from the corresponding author on reasonable request.

References

1. Cao YX, Xiao WH, Liu D, Zhang JL, Ding MZ, Yuan YJ. Biosynthesis of odd-chain fatty alcohols in Escherichia coli. Metab Eng. 2015;29:113-23; doi: 10.1016/j.ymben.2015.03.005.
2. Fatma Z, Jawed K, Mattam AJ, Yazdani SS. Identification of long chain specific aldehyde reductase and its use in enhanced fatty alcohol production in E. coli. Metab Eng. 2016;37:35-45; doi: 10.1016/j.ymben.2016.04.003.
3. Liu Y, Chen S, Chen J, Zhou J, Wang Y, Yang M, et al. High production of fatty alcohols in Escherichia coli with fatty acid starvation. Microb Cell Fact. 2016;15(1):129; doi: 10.1186/s12934-016-0524-5.
4. Sheng J, Stevens J, Feng X. Pathway Compartmentalization in Peroxisome of Saccharomyces cerevisiae to Produce Versatile Medium Chain Fatty Alcohols. Sci Rep. 2016;6:26884; doi: 10.1038/srep26884.

5. Munkajohnpong P, Kesornpun C, Buttranon S, Jaroensuk J, Weeranoppanant N, Chaiyen P. Fatty alcohol production: an opportunity of bioprocess. Biofuels, Bioproducts and Biorefining. 2020;14(5):986-1009; doi: 10.1002/bbb.2112.
6. Shah J, Arslan E, Cirucci J, O'Brien J, Moss D. Comparison of Oleo- vs Petro-Sourcing of Fatty Alcohols via Cradle-to-Gate Life Cycle Assessment. J Surfactants Deterg. 2016;19(6):1333-51; doi: 10.1007/s11743-016-1867-y.
7. Yeong SK, Idris Z, Hassan HA. 20 - Palm Oleochemicals in Non-food Applications. In: Lai O-M, Tan C-P, Akoh CC, editors. Palm Oil. AOCS Press; 2012. p. 587-624.
8. Liang SG, Liu HZ, Liu JL, Wang WT, Jiang T, Zhang ZF, et al. Hydrogenation of methyl laurate to produce lauryl alcohol over Cu/ZnO/Al2O3 with methanol as the solvent and hydrogen source. Pure Appl Chem. 2012;84(3):779-88; doi: 10.1351/PAC-CON-11-06-09.
9. Wu L, Moteki T, Gokhale Amit A, Flaherty David W, Toste FD. Production of Fuels and Chemicals from Biomass: Condensation Reactions and Beyond. Chem. 2016;1(1):32-58; doi: https://doi.org/10.1016/j.chempr.2016.05.002.
10. Munjal N, Jawed K, Wajid S, Yazdani SS. A constitutive expression system for cellulase secretion in Escherichia coli and its use in bioethanol production. PLoS One. 2015;10(3):e0119917; doi: 10.1371/journal.pone.0119917.
11. Munjal N, Mattam AJ, Pramanik D, Srivastava PS, Yazdani SS. Modulation of endogenous pathways enhances bioethanol yield and productivity in Escherichia coli. Microb Cell Fact. 2012;11:145; doi: 10.1186/1475-2859-11-145.
12. Choi YJ, Lee SY. Microbial production of short-chain alkanes. Nature. 2013;502(7472):571-4; doi: 10.1038/nature12536.
13. Kaiser BK, Carleton M, Hickman JW, Miller C, Lawson D, Budde M, et al. Fatty aldehydes in cyanobacteria are a metabolically flexible precursor for a diversity of biofuel products. PLoS One. 2013;8(3):e58307; doi: 10.1371/journal.pone.0058307.
14. Runguphan W, Keasling JD. Metabolic engineering of Saccharomyces cerevisiae for production of fatty acid-derived biofuels and chemicals. Metab Eng. 2014;21:103-13; doi: 10.1016/j.ymben.2013.07.003.
15. Xu P, Qiao K, Ahn WS, Stephanopoulos G. Engineering Yarrowia lipolytica as a platform for synthesis of drop-in transportation fuels and oleochemicals. Proceedings of the National Academy of Sciences. 2016;113(39):10848; doi: 10.1073/pnas.1607295113.
16. Coursolle D, Lian J, Shanklin J, Zhao H. Production of long chain alcohols and alkanes upon coexpression of an acyl-ACP reductase and aldehyde-deformylating oxygenase with a bacterial type-I fatty acid synthase in E. coli. Mol Biosyst. 2015;11(9):2464-72; doi: 10.1039/c5mb00268k.
17. Liu A, Tan X, Yao L, Lu X. Fatty alcohol production in engineered E. coli expressing Marinobacter fatty acyl-CoA reductases. Applied microbiology and biotechnology. 2013;97(15):7061-71; doi: 10.1007/s00253-013-5027-2.

18. Liu R, Zhu F, Lu L, Fu A, Lu J, Deng Z, et al. Metabolic engineering of fatty acyl-ACP reductase-dependent pathway to improve fatty alcohol production in Escherichia coli. Metab Eng. 2014;22:10-21; doi: 10.1016/j.ymben.2013.12.004.
19. Steen EJ, Kang Y, Bokinsky G, Hu Z, Schirmer A, McClure A, et al. Microbial production of fatty-acid-derived fuels and chemicals from plant biomass. Nature. 2010;463(7280):559-62; doi: 10.1038/nature08721.
20. Youngquist JT, Schumacher MH, Rose JP, Raines TC, Politz MC, Copeland MF, et al. Production of medium chain length fatty alcohols from glucose in Escherichia coli. Metabolic engineering. 2013;20:177-86; doi: 10.1016/j.ymben.2013.10.006.
21. Plapp BV, Leidal KG, Murch BP, Green DW. Contribution of liver alcohol dehydrogenase to metabolism of alcohols in rats. Chem Biol Interact. 2015;234:85-95; doi: 10.1016/j.cbi.2014.12.040.
22. Marsh ENG, Waugh MW. Aldehyde Decarbonylases: Enigmatic Enzymes of Hydrocarbon Biosynthesis. ACS Catalysis. 2013;3(11):2515-21; doi: 10.1021/cs400637t.
23. Jaroensuk J, Intasian P, Kiattisewee C, Munkajohnpon P, Chunthaboon P, Buttranon S, et al. Addition of formate dehydrogenase increases the production of renewable alkane from an engineered metabolic pathway. J Biol Chem. 2019;294(30):11536-48; doi: 10.1074/jbc.RA119.008246.
24. Aukema KG, Makris TM, Stoian SA, Richman JE, Münck E, Lipscomb JD, et al. Cyanobacterial aldehyde deformylase oxygenation of aldehydes yields n-1 aldehydes and alcohols in addition to alkanes. ACS Catal. 2013;3(10):2228-38; doi: 10.1021/cs400484m.
25. Schirmer A, Rude MA, Li X, Popova E, del Cardayre SB. Microbial biosynthesis of alkanes. Science (New York, NY). 2010;329(5991):559-62; doi: 10.1126/science.1187936.
26. Ichikawa S, Karita S. Bacterial production and secretion of water-insoluble fuel compounds from cellulose without the supplementation of cellulases. FEMS Microbiology Letters. 2015;362(24); doi: 10.1093/femsle/fnv202.
27. Krebs C, Bollinger JM, Jr., Booker SJ. Cyanobacterial alkane biosynthesis further expands the catalytic repertoire of the ferritin-like 'di-iron-carboxylate' proteins. Current opinion in chemical biology. 2011;15(2):291-303; doi: 10.1016/j.cbpa.2011.02.019.
28. Das D, Eser BE, Han J, Sciore A, Marsh EN. Oxygen-independent decarbonylation of aldehydes by cyanobacterial aldehyde decarbonylase: a new reaction of diiron enzymes. Angew Chem Int Ed Engl. 2011;50(31):7148-52; doi: 10.1002/anie.201101552.
29. Khara B, Menon N, Levy C, Mansell D, Das D, Marsh EN, et al. Production of propane and other short-chain alkanes by structure-based engineering of ligand specificity in aldehyde-deformylating oxygenase. Chembiochem. 2013;14(10):1204-8; doi: 10.1002/cbic.201300307.
30. Kurtz Jr DM. Structural similarity and functional diversity in diiron-oxo proteins. JBIC Journal of Biological Inorganic Chemistry. 1997;2(2):159-67; doi: 10.1007/s007750050120.
31. Merkx M, Kopp DA, Sazinsky MH, Blazyk JL, Müller J, Lippard SJ. Dioxygen Activation and Methane Hydroxylation by Soluble Methane Monooxygenase: A Tale of Two Irons and Three Proteins A list of abbreviations can be found in Section 7. Angew Chem Int Ed Engl. 2001;40(15):2782-807.

32. Akhtar MK, Turner NJ, Jones PR. Carboxylic acid reductase is a versatile enzyme for the conversion of fatty acids into fuels and chemical commodities. Proc Natl Acad Sci U S A. 2013;110(1):87-92; doi: 10.1073/pnas.1216516110.
33. Warui DM, Pandelia M-E, Rajakovich LJ, Krebs C, Bollinger JM, Booker SJ. Efficient Delivery of Long-Chain Fatty Aldehydes from the Nostoc punctiforme Acyl–Acyl Carrier Protein Reductase to Its Cognate Aldehyde-Deformylating Oxygenase. Biochemistry. 2015;54(4):1006-15; doi: 10.1021/bi500847u.
34. Li N, Nørgaard H, Warui DM, Booker SJ, Krebs C, Bollinger JM. Conversion of Fatty Aldehydes to Alka(e)nes and Formate by a Cyanobacterial Aldehyde Decarbonylase: Cryptic Redox by an Unusual Dimetal Oxygenase. Journal of the American Chemical Society. 2011;133(16):6158-61; doi: 10.1021/ja2013517.
35. Eser BE, Das D, Han J, Jones PR, Marsh ENG. Oxygen-independent alkane formation by non-heme iron-dependent cyanobacterial aldehyde decarbonylase: investigation of kinetics and requirement for an external electron donor. Biochemistry. 2011;50(49):10743-50; doi: 10.1021/bi2012417.
36. Li N, Chang W-c, Warui DM, Booker SJ, Krebs C, Bollinger JM. Evidence for Only Oxygenative Cleavage of Aldehydes to Alk(a/e)nes and Formate by Cyanobacterial Aldehyde Decarbonylases. Biochemistry. 2012;51(40):7908-16; doi: 10.1021/bi300912n.
37. Dennis M, Kolattukudy PE. A cobalt-porphyrin enzyme converts a fatty aldehyde to a hydrocarbon and CO. Proceedings of the National Academy of Sciences of the United States of America. 1992;89(12):5306-10; doi: 10.1073/pnas.89.12.5306.
38. Shanklin J, Guy JE, Mishra G, Lindqvist Y. Desaturases: emerging models for understanding functional diversification of diiron-containing enzymes. The Journal of biological chemistry. 2009;284(28):18559-63; doi: 10.1074/jbc.r900009200.
39. Friedle S, Reisner E, Lippard SJ. Current challenges of modeling diiron enzyme active sites for dioxygen activation by biomimetic synthetic complexes. Chemical Society Reviews. 2010;39(8):2768-79; doi: 10.1039/C003079C.
40. Nordlund P, Eklund H. Structure and function of the Escherichia coli ribonucleotide reductase protein R2. J Mol Biol. 1993;232(1):123-64; doi: 10.1006/jmbi.1993.1374.
41. Rosenzweig AC, Frederick CA, Lippard SJ, Nordlund P, auml. Crystal structure of a bacterial non-haem iron hydroxylase that catalyses the biological oxidation of methane. Nature. 1993;366(6455):537-43; doi: 10.1038/366537a0.
42. Elango N, Radhakrishnan R, Froland WA, Wallar BJ, Earhart CA, Lipscomb JD, et al. Crystal structure of the hydroxylase component of methane monooxygenase from Methylosinus trichosporium OB3b. Protein Sci. 1997;6(3):556-68; doi: 10.1002/pro.5560060305.
43. Mathevon C, Pierrel F, Oddou J-L, Garcia-Serres R, Blondin G, Latour J-M, et al. tRNA-modifying MiaE protein from Salmonella typhimurium is a nonheme diiron monooxygenase. Proceedings of the National Academy of Sciences. 2007;104(33):13295-300; doi: 10.1073/pnas.0704338104.

44. Lindqvist Y, Huang W, Schneider G, Shanklin J. Crystal structure of delta9 stearoyl-acyl carrier protein desaturase from castor seed and its relationship to other di-iron proteins. EMBO J. 1996;15(16):4081-92.
45. Newman LM, Wackett LP. Purification and characterization of toluene 2-monooxygenase from Burkholderia cepacia G4. Biochemistry. 1995;34(43):14066-76; doi: 10.1021/bi00043a012.
46. Crystal Structure of the Toluene/o-Xylene Monooxygenase Hydroxylase from Pseudomonas stutzeri OX1: INSIGHT INTO THE SUBSTRATE SPECIFICITY, SUBSTRATE CHANNELING, AND ACTIVE SITE TUNING OF MULTICOMPONENT MONOOXYGENASES. http://www.rcsb.org/structure/1T0R.
47. Pikus JD, Studts JM, Achim C, Kauffmann KE, Münck E, Steffan RJ, et al. Recombinant toluene-4-monooxygenase: catalytic and Mössbauer studies of the purified diiron and rieske components of a four-protein complex. Biochemistry. 1996;35(28):9106-19; doi: 10.1021/bi960456m.
48. Pandelia ME, Li N, Nørgaard H, Warui DM, Rajakovich LJ, Chang WC, et al. Substrate-triggered addition of dioxygen to the diferrous cofactor of aldehyde-deformylating oxygenase to form a diferric-peroxide intermediate. J Am Chem Soc. 2013;135(42):15801-12; doi: 10.1021/ja405047b.
49. Atsumi S, Wu TY, Eckl EM, Hawkins SD, Buelter T, Liao JC. Engineering the isobutanol biosynthetic pathway in Escherichia coli by comparison of three aldehyde reductase/alcohol dehydrogenase genes. Appl Microbiol Biotechnol. 2010;85(3):651-7; doi: 10.1007/s00253-009-2085-6.
50. Rajakovich LJ, Nørgaard H, Warui DM, Chang WC, Li N, Booker SJ, et al. Rapid Reduction of the Diferric-Peroxyhemiacetal Intermediate in Aldehyde-Deformylating Oxygenase by a Cyanobacterial Ferredoxin: Evidence for a Free-Radical Mechanism. J Am Chem Soc. 2015;137(36):11695-709; doi: 10.1021/jacs.5b06345.
51. Andre C, Kim SW, Yu X-H, Shanklin J. Fusing catalase to an alkane-producing enzyme maintains enzymatic activity by converting the inhibitory byproduct H₂O₂ to the cosubstrate O₂. Proceedings of the National Academy of Sciences. 2013;110(8):3191-6; doi: 10.1073/pnas.1218769110.
52. Meany JE, Pocker Y. The dehydration of glyoxalate hydrate: general-acid, general-base, metal ion and enzymic catalysis. Journal of the American Chemical Society. 1991;113(16):6155-61; doi: 10.1021/ja00016a035.
53. Ye Q, Hyndman D, Green N, Li X, Korithoski B, Jia Z, et al. Crystal structure of an aldehyde reductase Y50F mutant-NADP complex and its implications for substrate binding. Proteins: Structure, Function, and Bioinformatics. 2001;44(1):12-9; doi: 10.1002/prot.1066.
54. Gray CT, Wimpenny JW, Hughes DE, Mossman MR. Regulation of metabolism in facultative bacteria. I. Structural and functional changes in Escherichia coli associated with shifts between the aerobic and anaerobic states. Biochim Biophys Acta. 1966;117(1):22-32; doi: 10.1016/0304-4165(66)90148-6.
55. Das D, Ellington B, Paul B, Marsh ENG. Mechanistic Insights from Reaction of α-Oxiranyl-Aldehydes with Cyanobacterial Aldehyde Deformylating Oxygenase. ACS Chemical Biology. 2014;9(2):570-7; doi: 10.1021/cb400772q.

56. Gao Y, Zhang H, Fan M, Jia C, Shi L, Pan X, et al. Structural insights into catalytic mechanism and product delivery of cyanobacterial acyl-acyl carrier protein reductase. Nature Communications. 2020;11(1):1525; doi: 10.1038/s41467-020-15268-y.
57. Wang Q, Bao L, Jia C, Li M, Li J-J, Lu X. Identification of residues important for the activity of aldehyde-deformylating oxygenase through investigation into the structure-activity relationship. BMC Biotechnology. 2017;17(1):31; doi: 10.1186/s12896-017-0351-8.
58. Bao L, Li J-J, Jia C, Li M, Lu X. Structure-oriented substrate specificity engineering of aldehyde-deformylating oxygenase towards aldehydes carbon chain length. Biotechnology for Biofuels. 2016;9(1):185; doi: 10.1186/s13068-016-0596-9.
59. Zhang L, Liang Y, Wu W, Tan X, Lu X. Microbial synthesis of propane by engineering valine pathway and aldehyde-deformylating oxygenase. Biotechnology for Biofuels. 2016;9(1):80; doi: 10.1186/s13068-016-0496-z.
60. Åberg A, Nordlund P, Eklund H. Unusual clustering of carboxyl side chains in the core of iron-free ribonucleotide reductase. Nature. 1993;361(6409):276-8; doi: 10.1038/361276a0.
61. Menon N, Pásztor A, Menon BRK, Kallio P, Fisher K, Akhtar MK, et al. A microbial platform for renewable propane synthesis based on a fermentative butanol pathway. Biotechnology for Biofuels. 2015;8(1):61; doi: 10.1186/s13068-015-0231-1.
62. Patrikainen P, Carbonell V, Thiel K, Aro E-M, Kallio P. Comparison of orthologous cyanobacterial aldehyde deformylating oxygenases in the production of volatile C3-C7 alkanes in engineered E. coli. Metab Eng Commun. 2017. doi: 10.1016/j.meteno.2017.05.001.
63. Harger M, Zheng L, Moon A, Ager C, An JH, Choe C, et al. Expanding the Product Profile of a Microbial Alkane Biosynthetic Pathway. ACS Synthetic Biology. 2013;2(1):59-62; doi: 10.1021/sb300061x.
64. Kallio P, Pásztor A, Thiel K, Akhtar MK, Jones PR. An engineered pathway for the biosynthesis of renewable propane. Nature Communications. 2014;5(1):4731; doi: 10.1038/ncomms5731.
65. Buer BC, Paul B, Das D, Stuckey JA, Marsh ENG. Insights into substrate and metal binding from the crystal structure of cyanobacterial aldehyde deformylating oxygenase with substrate bound. ACS chemical biology. 2014;9(11):2584-93; doi: 10.1021/cb500343j.
66. Dolinsky TJ, Nielsen JE, McCammon JA, Baker NA. PDB2PQR: an automated pipeline for the setup of Poisson–Boltzmann electrostatics calculations. Nucleic Acids Research. 2004;32(suppl_2):W665-W7; doi: 10.1093/nar/gkh381.
67. MacKerell AD, Bashford D, Bellott M, Dunbrack RL, Evanseck JD, Field MJ, et al. All-atom empirical potential for molecular modeling and dynamics studies of proteins. J Phys Chem B. 1998;102(18):3586-616; doi: 10.1021/jp973084f.
68. Phillips JC, Braun R, Wang W, Gumbart J, Tajkhorshid E, Villa E, et al. Scalable molecular dynamics with NAMD. J Comput Chem. 2005;26(16):1781-802; doi: 10.1002/jcc.20289.
69. Pongpamorn P, Watthaisong P, Pimviriyakul P, Jaruwat A, Lawan N, Chitnumsub P, et al. Identification of a Hotspot Residue for Improving the Thermostability of a Flavin-Dependent Monooxygenase. ChemBioChem. 2019;20(24):3020-31; doi: 10.1002/cbic.201900413.

70. Phillips J, Isgro T, Sotomayor M, Villa E, Yu H, Tanner D, et al. NAMD tutorial. 2012.

71. Isgro T, Phillips J, Sotomayor M, Villa E, Yu H, Tanner D, et al. NAMD tutorial. 2017.

Tables

Table 1. Yields of the corresponding alkane, acid, and alcohol products obtained from dodecanal conversion by *Pm*ADO catalysis under various $\%O_2$ in the presence and absence of the reducing partner.

*Pm*ADO reaction	$\%O_2$	Alkane[a] (μM)	Acid[b] (μM)	Alcohol[b] (μM)
With Fd/FNR (+NADPH)	<0.0004	N.D.	N.D.	75 ± 4
	10	5 ± 2	11 ± 3	13 ± 8
	15	6 ± 2	32 ± 2	6 ± 1
Without Fd/FNR (+NADPH)	<0.0004	N.D.	N.D.	69 ± 5
	10	N.D.	19 ± 8	10 ± 3
	15	N.D.	36 ± 4	9 ± 2

[a]The product formed with one carbon less (C_{n-1}).

[b]The product formed with a full-chain length.

N.D., not detectable

Table 2. Kinetic parameters of *Pm*ADO reductase activity towards C_6, C_8, C_{10}, C_{12}, and C_{14} aldehydes.

Aldehydes	k_{cat} (min^{-1})	K_m (μM)	k_{cat}/K_m ($\mu M^{-1}min^{-1}$)
C_6	0.10	10.78 ± 2.51	10×10^{-3}
C_8	0.14	10.26 ± 0.88	14×10^{-3}
C_{10}	0.10	6.52 ± 1.57	15×10^{-3}
C_{12}	0.05	15.87 ± 3.72	3×10^{-3}
C_{14}	0.06	12.06 ± 1.25	5×10^{-3}

Figures

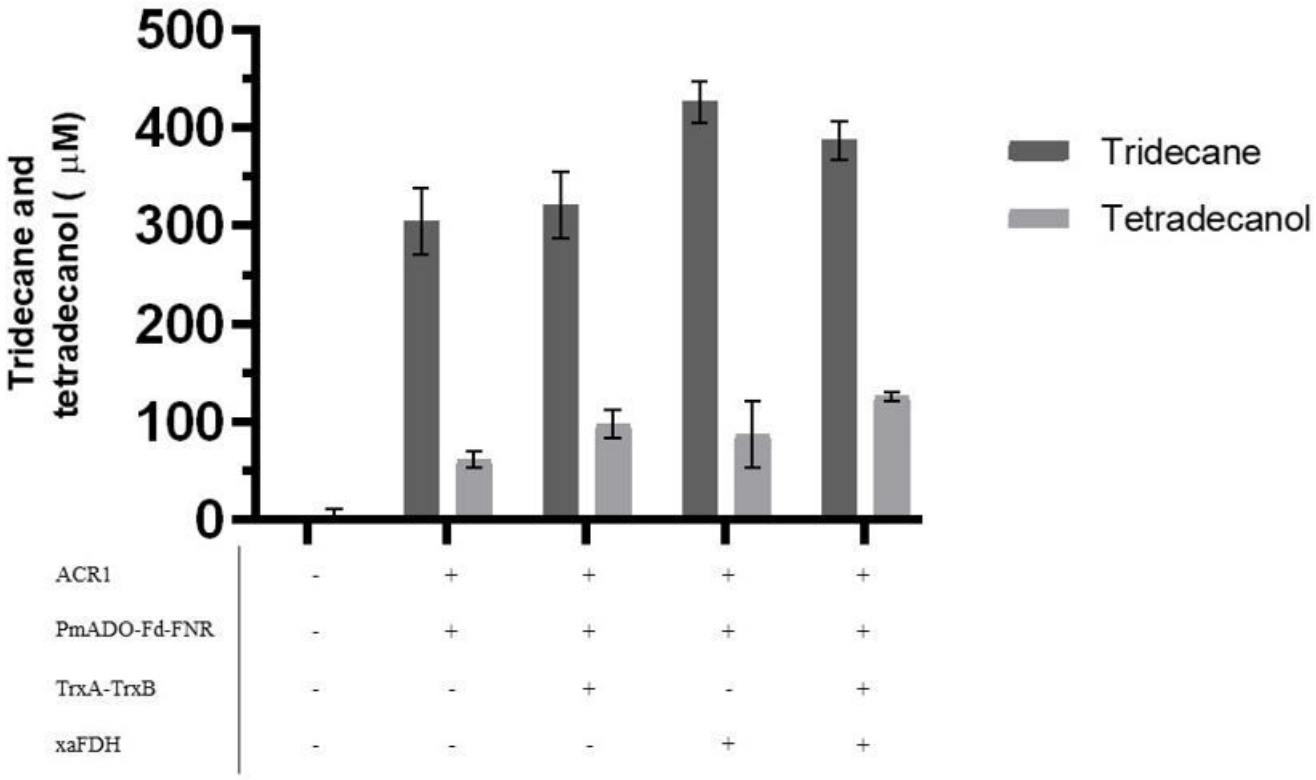

Figure 1

Alkane and fatty alcohol production in whole cell biocatalysis. The measured concentrations of tridecane and tetradecanol in five cell types containing different sets of genes. Data represent the mean ± SD (n=3).

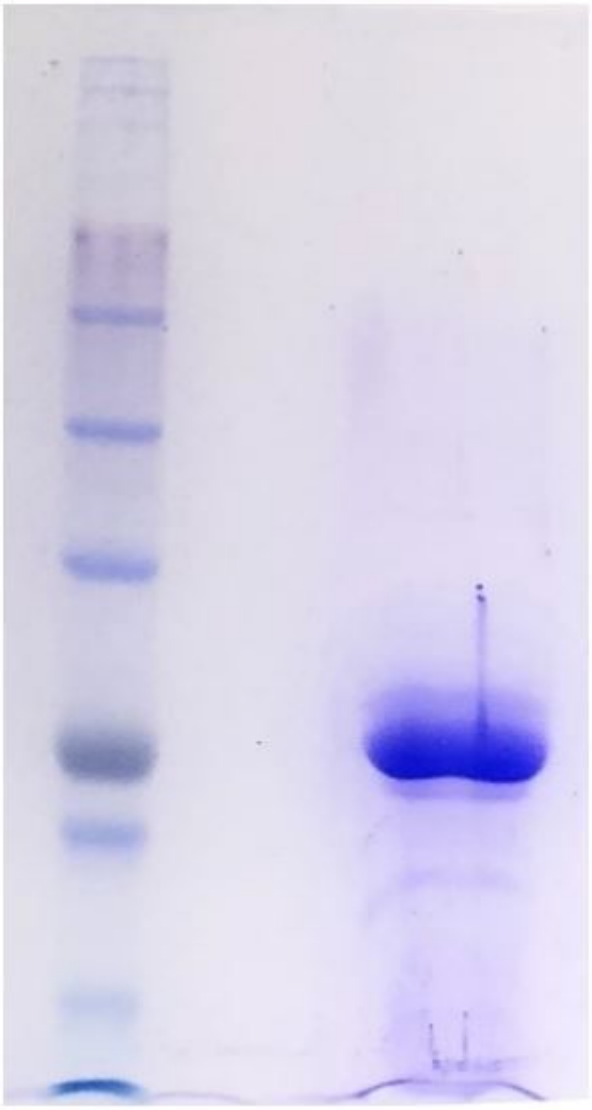

Figure 2

SDS-PAGE. The result shows the purity of PmADO that has a molecular weight subunit approximately 24 kDa.

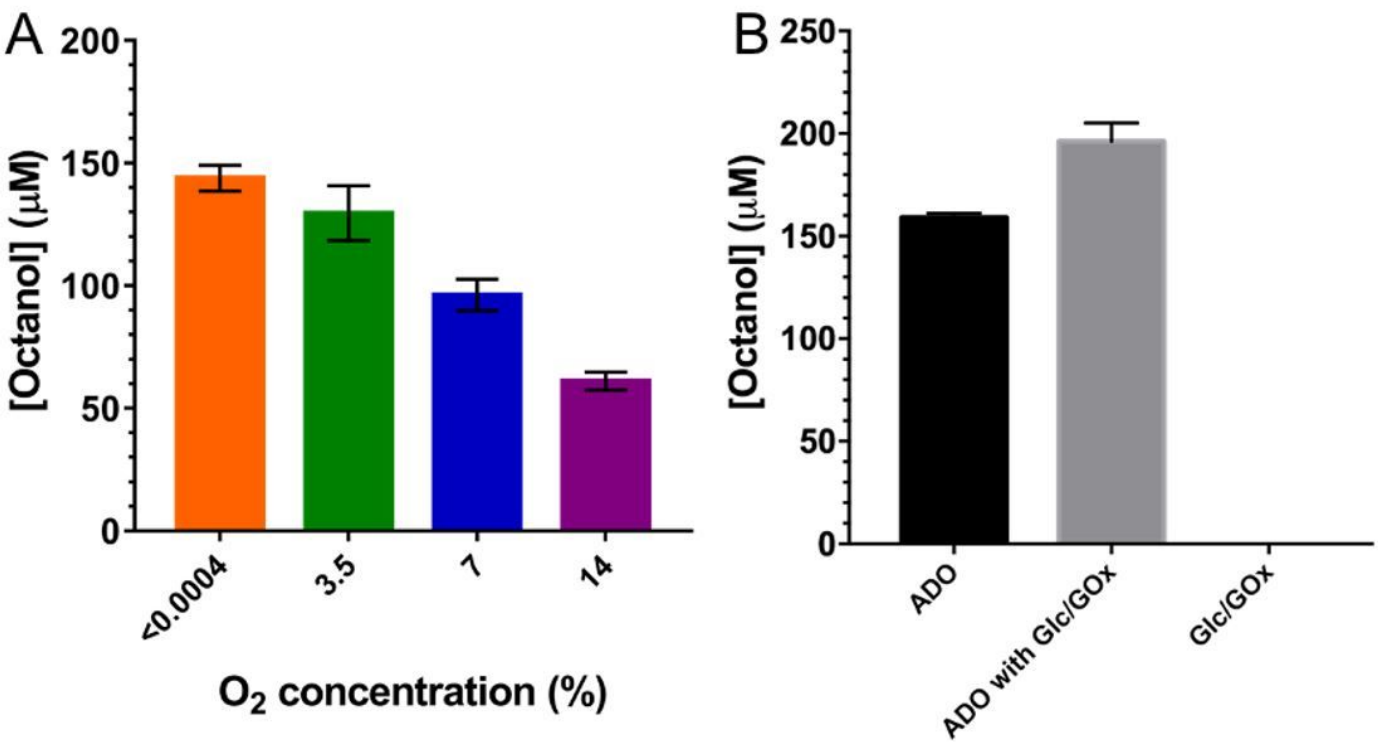

Figure 3

Effects of O2 on alcohol production in the reaction using octanal as a substrate. (A) The measured concentration of octanol produced from the NADPH-utilizing reduction of octanal (250 μM) by PmADO in the presence of different %O2 including <0.0004 (orange), 3.5 (green), 7 (blue) and 14 (purple). (B) Octanol production by PmADO in the presence (grey) or absence (black) of 200 μM Glc and 10 μg/ml GOx as an oxygen scavenging system. Data represent the mean ± SD (n=3).

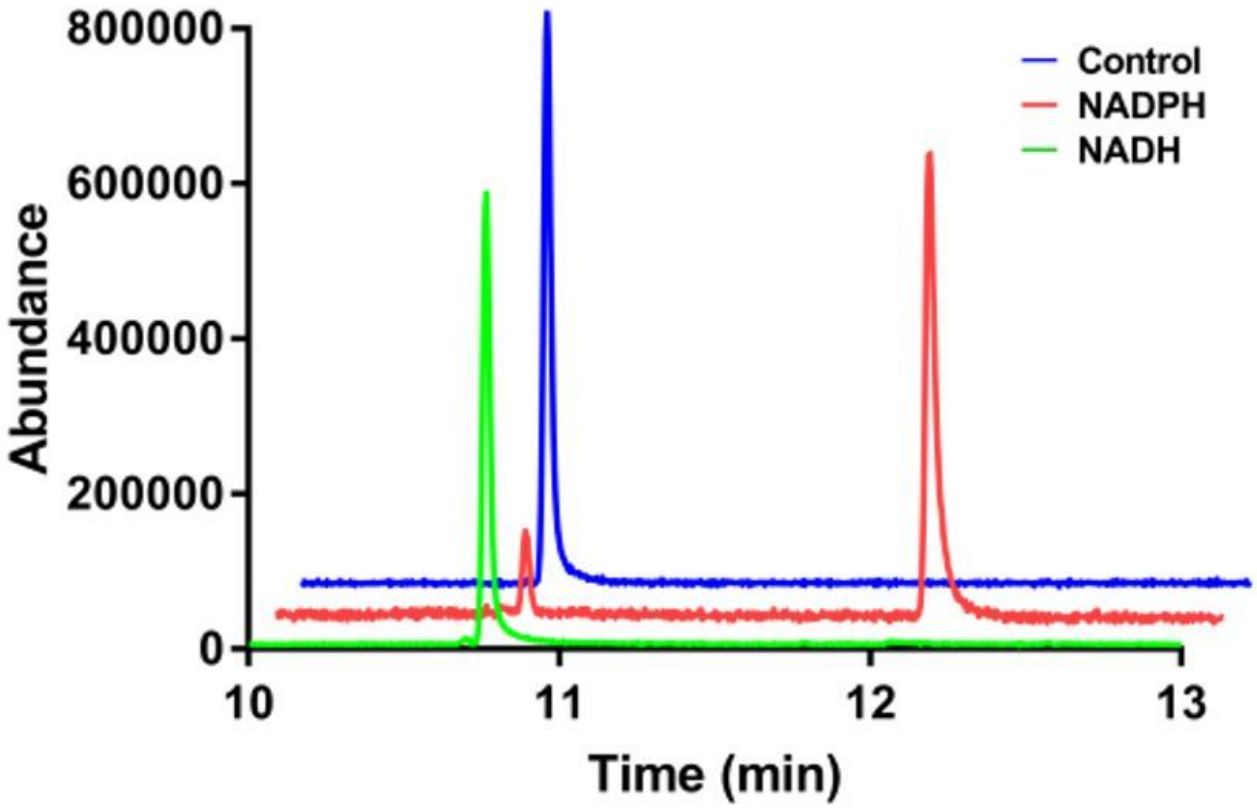

Figure 4

The GC-MS chromatograms in the reaction of PmADO with NADH and NADPH. The reaction with NADH (green) shows only octanal as a substrate at retention time 10.8 min with no alcohol production. The control reaction without reducing agent added also shows the same octanal as a substrate (blue). Only the reaction with NADPH (red) shows formation of octanol (retention time at 12.2 minute).

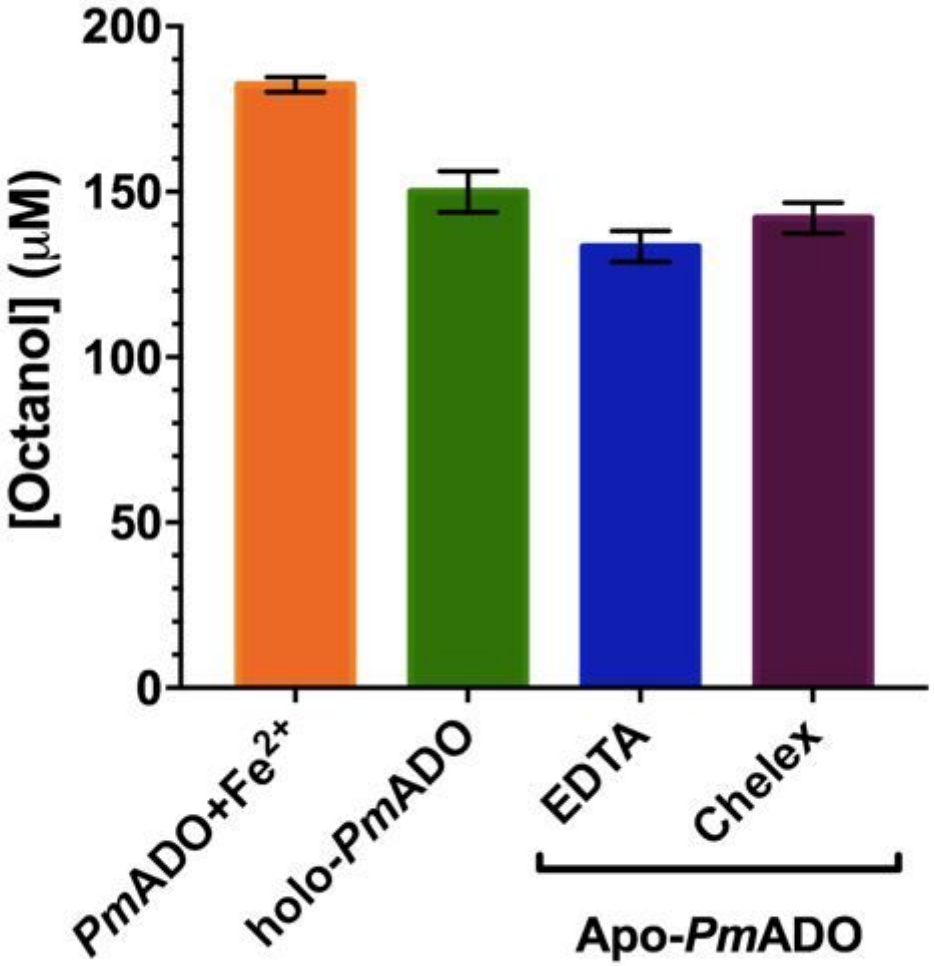

Figure 5

Effect of Fe2+ on alcohol production. Amount of octanol in PmADO reactions supplemented with Fe2+ (orange), holo-PmADO (Green), apo-PmADO prepared by EDTA (blue) and chelating gel (purple) methods. The amount of metal in each experiment was observed using ICP-OES, which reports the mole ratio of PmADO and Fe2+, 1:2 in PmADO + Fe2+, 1:0.1 in apo-PmADO. Data represent the mean ± SD (n=3).

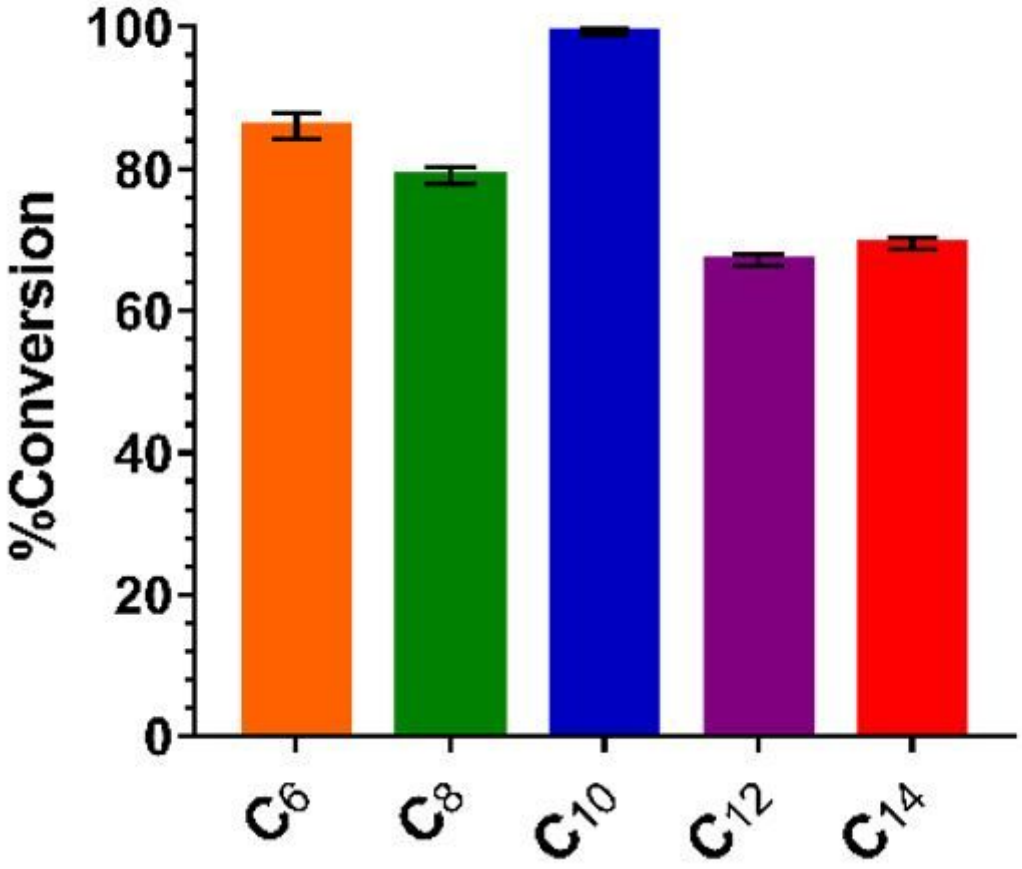

Figure 6

Substrate specificity of PmADO reductase activity on alcohol production. The %conversion of several substrates for PmADO, including hexanal (orange), octanal (green), decanal (blue), dodecanal (purple) and tetradecanal (red).

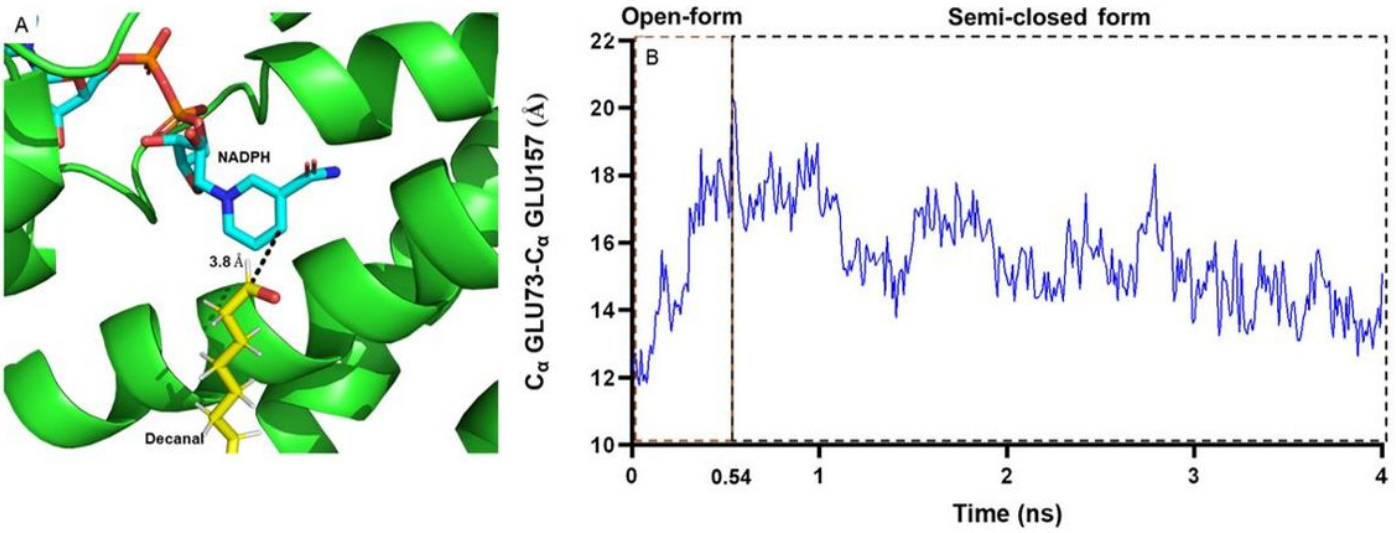

Figure 7

Docking-MD simulations on NADPH binding to PmADO enzyme with decanal substrate. Docking-MD results from 0.54 ns equilibration of PmADO with NADPH and decanal show distant between nicotinamide ring to carbonyl carbon of aldehyde around 3.8 Å (A). Cα Glu73-Cα Glu157 distances during 4 ns MD simulations for PmADO enzyme with NADPH and decanal (B).

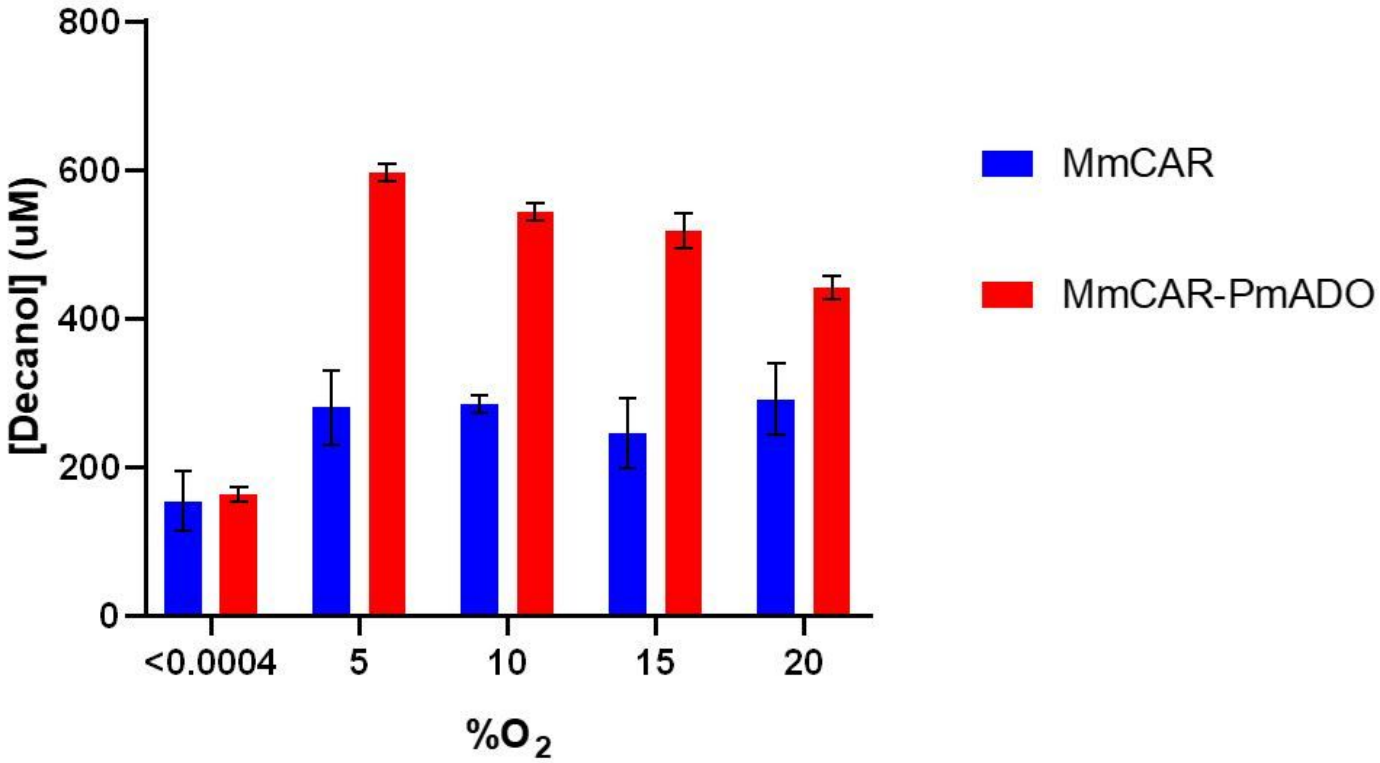

Figure 8

Effect of O2 on decanol production in whole cell biocatalysis. The measured concentration of decanol in various concentrations of O2 between 2 cell types, E. coli BL21(DE3) containing MmCAR (blue) and E. coli BL21(DE3) containing MmCAR/PmADO (red), at 6 hours.

Supplementary Files

This is a list of supplementary files associated with this preprint. Click to download.

- Additionalfiles1.docx
- Scheme1.JPG